

Carlo Bartolozzi
Francescamaria Donati
Dania Cioni
Carlo Procacci
Giovanni Morana
Antonio Chiesa
Luigi Grazioli
Giorgio Cittadini
Giuseppe Cittadini
Andrea Giovagnoni
Giovanni Gandini
Jochen Maass
Riccardo Lencioni

Received: 17 March 2003
Accepted: 2 May 2003
Published online: 9 August 2003
© Springer-Verlag 2003

C. Bartolozzi (✉) · F. Donati · D. Cioni
R. Lencioni
Department of Radiology,
University of Pisa,
Via Roma 67, 56100 Pisa, Italy
e-mail: Bartolozzi@do.med.unipi.it
Tel.: +39-050-992509
Fax: +39-050-551461

C. Procacci · G. Morana
Department of Radiology,
University of Verona,
Piazzale L.A. Scuro 1, 37134 Verona, Italy

A. Chiesa · L. Grazioli
Department of Radiology,
University of Brescia,
Piazzale Spedali Civili 1, 25023 Brescia,
Italy

G. Cittadini · G. Cittadini
Department of Radiology,
University of Genova,
Largo R. Benzi 10, 16132 Genova, Italy

Detection of colorectal liver metastases: a prospective multicenter trial comparing unenhanced MRI, MnDPDP-enhanced MRI, and spiral CT

A. Giovagnoni
Department of Radiology,
University of Ancona,
Concam, Torrette, 60020 Ancona, Italy

G. Gandini · J. Maass
Department of Radiology,
University of Torino,
Genova 3, 10110 Torino, Italy

Abstract The aim of this study was to compare unenhanced MRI, MnDPDP-enhanced MRI, and spiral CT in the detection of hepatic colorectal metastases. Forty-four patients with hepatic colorectal metastases were examined with unenhanced and MnDPDP-enhanced MRI and with unenhanced and contrast-enhanced spiral CT. The MR examination protocol included baseline T1-weighted spin-echo (SE), T1-weighted gradient-recalled-echo (GRE), and T2-weighted fast-SE sequences; and T1-weighted SE and T1-weighted GRE sequences obtained 30–60 min after administration of 0.5 $\mu\text{mol/kg}$ (0.5 ml/kg) mangafodipir trisodium (MnDPDP). Images were interpreted

by three blinded readers. Findings at CT and MRI were compared with those at intraoperative US, which were used as term of reference. Intraoperative US detected 128 metastases. In a lesion-by-lesion analysis, the overall detection rate was 71% (91 of 128) for spiral CT, 72% (92 of 128) for unenhanced MRI, and 90% (115 of 128) for MnDPDP-enhanced MRI. MnDPDP-enhanced MRI was more sensitive than either unenhanced MRI ($p<0.0001$) or spiral CT ($p=0.0007$). In a patient-by-patient analysis, agreement with gold standard was higher for MnDPDP-enhanced MRI (33 of 44 cases) than for spiral CT (22 of 44 cases, $p=0.0023$) and unenhanced MRI (21 of 44 cases, $p=0.0013$). MnDPDP-enhanced MRI is superior to unenhanced MRI and spiral CT in the detection of hepatic colorectal metastases.

Keywords Liver neoplasms · Computed tomography · Metastases · Magnetic resonance · Contrast media · Mangafodipir trisodium

Introduction

Metastatic disease in the liver usually indicates advanced disease and a poor prognosis. In patients with hepatic metastases from primary malignancies developed in the gastrointestinal tract, particularly colorectal adenocarcinoma, a substantial improvement in long-term survival can be achieved with surgical removal or percutaneous

ablation of the metastatic burden [1, 2, 3, 4, 5]. A 5-year survival rate of approximately 20–40% and a 5-year disease-free survival rate of approximately 20–25%, in fact, can be expected in successfully treated patients [6, 7].

The success of surgery and tumor ablation therapies depends on the knowledge of the exact number and location of metastatic lesions [7]. Several CT and MR examination protocols have been used for preoperative detec-

tion of liver metastases [8, 9, 10]. In MRI, efforts aimed at enhancing lesion detectability have been especially focused on the development of tissue-specific contrast agents, including reticulo-endothelial-system-targeted agents and hepatobiliary agents [11, 12].

Mangafodipir trisodium is a paramagnetic hepatobiliary MR contrast agent. Following intravenous administration, Mn is taken up by the hepatocytes. This leads, as a consequence of T1-shortening, to an increased signal intensity of normal hepatic parenchyma, thus enhancing contrast between liver and focal lesions. Several studies have investigated the usefulness of MRI after administration of MnDPDP [13, 14, 15, 16, 17, 18, 19]. There appears to be consensus that MnDPDP-enhanced MRI improves lesion conspicuity and increases lesion detection rate. The role of MnDPDP-enhanced MRI with respect to spiral CT in the preoperative assessment of patients with liver metastases, however, has not been fully defined. The purpose of this study was to compare MnDPDP-enhanced MRI with spiral CT for the detection of hepatic colorectal metastases in a series of patients who were candidates for surgical resection or intraoperative radio-frequency thermal ablation.

Materials and methods

The study was designed as a prospective, multi-institutional trial. The primary end point of the study was to compare the sensitivity of unenhanced and Mn-DPDP-enhanced MRI with that of spiral CT in the detection of hepatic colorectal metastases in lesion-by-lesion and patient-by-patient analyses. Secondary end points included the assessment of (a) lesion conspicuity, (b) quality of lesion delineation, and (c) confidence in diagnosis in each unenhanced or enhanced MR pulse sequence and in spiral CT images.

Inclusion criteria were: (a) adult patient with hepatic colorectal cancer metastasis; (b) patient scheduled for partial hepatectomy or intra-operative radio-frequency thermal ablation; and (c) signed written informed consent. Exclusion criteria were: (a) pregnant or lactating woman; (b) inclusion in other investigational study in the 7 days prior to the enrollment; (c) severe obstructive biliary disease or renal insufficiency; (d) severe hepatic dysfunction (Child class C); and (e) general contraindication to MRI.

A series of 44 consecutive adult patients with hepatic colorectal metastases, referred to the participating centers for pre-operative imaging assessment, were included in the study. Twenty-two patients were enrolled in Pisa, 7 in Verona, 6 in Brescia, 5 in Genoa, 2 in Ancona, and 2 in Turin. All patients underwent unenhanced and MnDPDP-enhanced MRI at 0.5 T ($n=8$), 1.0 T ($n=6$), or 1.5 T ($n=30$) as well as unenhanced and contrast-enhanced spiral CT.

Magnetic resonance examination protocol included baseline T1-weighted SE and GRE sequences and T2-weighted fast-spin-echo (FSE) sequences. The T1-weighted SE and GRE sequences were then repeated 30–60 min following IV infusion of 0.5 $\mu\text{mol/kg}$ (0.5 ml/kg) MnDPDP (Teslascan, Amersham Health, Oslo, Norway) at the rate of 2.5 ml/min. In each center, the routine parameters used for liver MR studies were used. Also, unenhanced and contrast-enhanced CT studies were optimized for liver metastasis detection according to the standard examination protocol adopted in each center.

All patients underwent either partial hepatectomy or intraoperative radio-frequency thermal ablation. Gold standard was

provided by findings at visual inspection of the liver surface and intraoperative US. Lesions which were identified for the first time at intraoperative US were resected whenever possible together with the known tumor. In resected cases, findings at intraoperative US were then matched with those at pathology examination of the surgical specimen. If lesions identified at intraoperative US were in locations that made hepatic resection inappropriate, they were treated intraoperatively by US-guided radio-frequency thermal ablation.

Images were interpreted blindly and prospectively by three readers who were asked to reach a consensus. For the primary end point of the study, the readers evaluated three sets of images for each patient. The first set contained baseline T1-weighted SE, T1-weighted GRE, and T2-weighted FSE sequences; the second set contained baseline T1-weighted SE, T1-weighted GRE, and T2-weighted FSE sequences plus MnDPDP-enhanced T1-weighted SE and T1-weighted GRE sequences; and the third set contained unenhanced plus contrast-enhanced spiral CT images. For the secondary end points of the study, each MR pulse sequence was then evaluated separately. Lesion conspicuity and quality of lesion delineation were graded as: absent; poor; moderate; or excellent. The level of confidence in the diagnosis was graded as: not very confident; moderately confident; very confident; or extremely confident.

The statistical analysis of the results was performed using the McNemar test and the Wilcoxon t test for paired data. A p value less than 0.05 was considered statistically significant.

Results

Findings at intraoperative US showed 128 metastatic lesions, ranging 0.2–12.0 cm in diameter. Forty seven of 128 lesions were smaller than or equal to 1 cm in diameter, 31 ranged 1.1–2 cm, and 45 were larger than 2 cm. Pathologic confirmation of metastasis was achieved in 89 of 128 lesions that were surgically resected. The remaining 39 of 128 lesions were submitted to intra-operative radio-frequency thermal ablation.

In the lesion-by-lesion analysis, the overall detection rate was 71% (91 of 128 lesions) for spiral CT, 72% (92 of 128) for unenhanced MRI, and 90% (115 of 128) for MnDPDP-enhanced MRI. MnDPDP-enhanced MRI was more sensitive than either unenhanced MRI ($p<0.0001$) or spiral CT ($p=0.0007$; Figs. 1, 2, 3). In lesions ≤ 1 cm in diameter, the difference in sensitivity among spiral CT (38%), unenhanced MRI (51%), and MnDPDP-enhanced MRI (83%) was even more manifest (Table 1). All lesions undetected by MnDPDP-enhanced MRI and discovered at the time of surgery by intraoperative US did not exceed 1 cm in diameter.

In the patient-by-patient analysis, agreement with gold standard in assessing the hepatic metastatic tumor burden was higher for MnDPDP-enhanced MRI (33 of 44 cases) than for spiral CT (22 of 44 cases, $p=0.0023$) and unenhanced MRI (21 of 44 cases, $p=0.0013$). Underestimation of lesions (false negatives) were observed in 19 patients at spiral CT, in 21 patients at unenhanced MRI, and in 9 patients at MnDPDP-enhanced MRI. Overestimation of lesions (false positives) were observed in 3 patients at spiral CT, in 2 patients at unenhanced

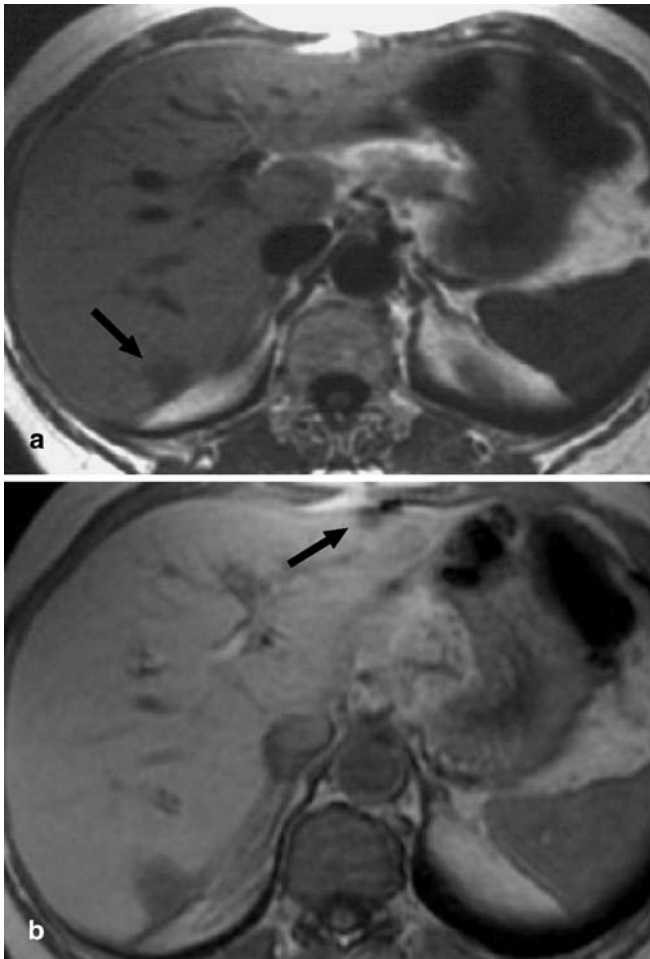


Fig. 1 **a** Unenhanced T1-weighted MR image shows solitary metastasis in segment VII (*arrow*). **b** After injection of mangafodipir trisodium (MnDPDP), lesion conspicuity is increased, and a second metastasis, undetected by baseline MR examination, is observed in the anterior subcapsular aspect of segment III (*arrow*)



Fig. 2 **a** Contrast-enhanced spiral CT fails to show any lesion in the level shown. **b** MnDPDP-enhanced T1-weighted gradient-recalled-echo (GRE) MR image shows tiny metastasis <1 cm in greatest dimension (*arrow*)

Table 1 Comparison among unenhanced MRI, MnDPDP-enhanced MRI, and spiral CT in the detection of hepatic colorectal metastases in a lesion-by-lesion analysis according to lesion size

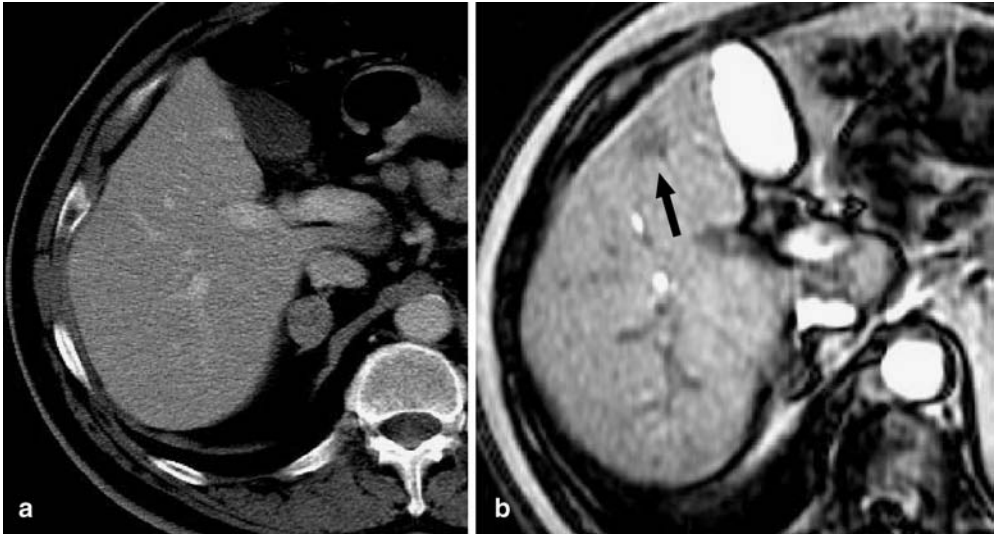
Imaging study	No. of lesions detected/studied			Overall
	≤1 cm	1.1–2 cm	>2 cm	
Spiral CT	18/47 (38)	28/31 (90)	45/45 (100)	91/128 (71)
Unenhanced MRI	24/47 (51)	24/31 (77)	44/45 (98)	92/128 (72)
Enhanced MRI ^a	39/47 (83)	31/31 (100)	45/45 (100)	115/128 (90) ^b

Numbers in parentheses are percentages

^a Enhanced MRI includes baseline and MnDPDP-enhanced sequences

^b Enhanced MRI was significantly more sensitive than either unenhanced MRI ($p < 0.0001$) or spiral CT ($p = 0.0007$). The Wilcoxon t test for paired data was used for statistical analysis

Fig. 3 **a** Contrast-enhanced spiral CT does not show any focal abnormality. **b** MnDPDP-enhanced T1-weighted GRE MR image shows a 1-cm metastasis in segment V (*arrow*). Right adrenal adenoma is also detected



MRI, and in 2 patients at MnDPDP-enhanced MRI (Table 2). Lesions overestimated as metastases were diagnosed as hemangioma ($n=1$) or cyst ($n=2$) intraoperatively.

Lesion conspicuity, quality of lesion delineation, and confidence in diagnosis were all significantly higher for

post-contrast T1-weighted GRE images than any other pre-contrast or post-contrast MR images or for spiral CT images (Tables 3, 4, 5).

Table 2 Comparison among unenhanced MRI, MnDPDP-enhanced MRI, and spiral CT in the assessment of the hepatic metastatic tumor burden in a patient-by-patient analysis

Imaging study	Comparison with intraoperative US findings		
	Underestimation of lesions	Agreement	Overestimation of lesions
Spiral CT	19/44 (43)	22/44 (50)	3/44 (7)
Unenhanced MRI	20/44 (45)	22/44 (50)	2/44 (5)
Enhanced MRI ^a	9/44 (20)	33/44 (75) ^b	2/44 (5)

Numbers are numbers of patients. Numbers in parentheses are percentages

^a Enhanced MRI includes baseline and MnDPDP-enhanced sequences

^b Enhanced MRI was significantly more accurate than either unenhanced MRI ($p=0.0013$) or spiral CT ($p=0.0023$). The McNemar test was used for statistical analysis

Discussion

Many studies have compared different imaging modalities or different methods or examination protocols within the same modality in attempts to optimize detection of colorectal liver metastases, particularly in patients who are candidates for partial hepatectomy. Until recently, the general opinion was that CT during arterial portography was the best preoperative method for the detection of hepatic metastases, with a sensitivity ranging between 89 and 94% in series in which surgical confirmation was obtained [20, 21, 22, 23]. Computed tomographic arterial portography, however, is an invasive procedure that requires angiography. Moreover, it has a high false-positive rate, due to the presence of benign liver tumors—such as hemangiomas, nontumorous portal vein perfusion defects, and small cysts, all of which may simulate tumor [22].

With improvements in hardware and software, MRI has in recent years assumed an important role in the

Table 3 Lesion conspicuity in unenhanced MR images, MnDPDP-enhanced MR images, and spiral CT images. *SE* spin echo, *GRE* gradient-recalled echo, *FSE* fast spin echo

	Absent	Poor	Moderate	Excellent	Not assessed
Spiral CT	–	6 (6.6)	39 (42.9)	46 (50.6)	–
Unenhanced T1-weighted SE	1 (1.3)	21 (28.0)	42 (56.0)	11 (14.7)	–
Unenhanced T1-weighted GRE	–	13 (14.1)	51 (55.4)	28 (30.4)	–
Unenhanced T2-weighted FSE	–	15 (17.2)	43 (49.4)	28 (32.2)	1 (1.2)
MnDPDP-enhanced T1-weighted SE	–	13 (14.6)	38 (42.7)	38 (42.7)	–
MnDPDP-enhanced T1-weighted GRE	–	–	19 (16.5)	96 (83.5)	–

Numbers in parentheses are percentages

Table 4 Quality of lesion delineation in unenhanced MR images, MnDPDP-enhanced MR images, and spiral CT images

	Absent	Poor	Moderate	Excellent	Not assessed
Spiral CT	1 (1.1)	6 (6.6)	46 (50.6)	38 (41.8)	–
Unenhanced T1-weighted SE	2 (2.7)	23 (30.7)	42 (56)	8 (10.7)	–
Unenhanced T1-weighted GRE	–	19 (20.6)	47 (51.1)	25 (27.2)	1 (1.1)
Unenhanced T2-weighted FSE	–	20 (23.0)	42 (48.3)	24 (27.6)	1 (1.2)
MnDPDP-enhanced T1-weighted SE	12 (13.5)	25 (28.1)	23 (25.8)	29 (32.6)	–
MnDPDP-enhanced T1-weighted GRE	–	3 (2.6)	17 (14.8)	94 (81.7)	1 (0.9)

Numbers in parentheses are percentages

Table 5 Diagnostic confidence in unenhanced MR images, MnDPDP-enhanced MR images, and spiral CT images

	Not very confident	Moderately confident	Very confident	Extremely confident	Not assessed
Spiral CT	4 (3.1)	14 (10.9)	36 (28.1)	36 (28.1)	1 (1.1)
Unenhanced T1-weighted SE	20 (26.7)	24 (32.0)	17 (22.7)	14 (18.7)	–
Unenhanced T1-weighted GRE	15 (16.3)	23 (25.0)	28 (30.4)	26 (28.3)	–
Unenhanced T2-weighted FSE	14 (16.1)	28 (32.2)	23 (26.4)	22 (25.3)	–
MnDPDP-enhanced T1-weighted SE	12 (13.5)	25 (28.1)	23 (25.8)	29 (32.6)	–
MnDPDP-enhanced T1-weighted GRE	1 (0.9)	14 (12.2)	15 (13.0)	84 (73.0)	1 (0.9)

Numbers in parentheses are percentages

evaluation of the liver for focal diseases. The sensitivity of unenhanced MRI, however, is considered to be equal or at best only marginally higher than that of contrast-enhanced CT [11]. Moreover, MRI enhanced with extracellular contrast agents, i.e., gadolinium chelates, showed no improvement over unenhanced MRI in detectability of liver metastases, particularly when blinded readers from different institutions were used [24, 25, 26]. In one study, the number of false-positive and false-negative diagnoses of individual lesions were higher with dynamic gadolinium-enhanced MR images than with unenhanced images [26].

With the advent of tissue-specific MR contrast media, investigation has been focused on assessing the value of MRI after administration of reticulo-endothelial-system-targeted agents, such as ferumoxides, or hepatobiliary agents for the detection of focal liver lesions. Previous studies have shown the usefulness of ferumoxides-enhanced MRI for increasing tumor-to-liver contrast and improving lesion conspicuity on T2-weighted images [27, 28, 29]. In one series, ferumoxides-enhanced MRI was at least as accurate as CT arterial portography for the detection of hepatic metastases [30]. In two comparisons of MR imaging findings with the results of intraoperative US and pathologic examination, the sensitivity of ferumoxides-enhanced MRI ranged from 56 to 83% [23, 31].

In this study, we compared MRI with administration of the hepatobiliary agent MnDPDP with spiral CT for the detection of hepatic colorectal metastases in a series of patients who were candidates for surgical resection or intraoperative radio-frequency thermal ablation and in

whom intraoperative US findings could be used as term of reference. In a lesion-by-lesion analysis, MRI significantly outperformed spiral CT and unenhanced MRI in the detection of metastatic deposits. The overall sensitivity of MnDPDP-enhanced MRI reached 90% as opposed to 71% for spiral CT and 72% of unenhanced MRI. The difference in the detection rate between MnDPDP-enhanced MRI and spiral CT was even more manifest when only lesions ≤ 1 cm in diameter were considered: in this group, MnDPDP-enhanced MRI showed a sensitivity of 83% as opposed to 38% of spiral CT and 51% of unenhanced MRI.

Analysis of our data on a patient-by-patient basis confirmed the superiority of MnDPDP-enhanced MRI over baseline MRI and spiral CT. While the extent of the hepatic metastatic burden was underestimated or overestimated in half of the patients by unenhanced MRI and spiral CT, findings at MnDPDP-enhanced MRI were in agreement with those at intraoperative US in 75% of the cases. Nevertheless, either false-negative or, occasionally, false-positives lesions occurred in the remaining 25% of patients even with use of MnDPDP-enhanced MRI. Our findings confirm, in a larger series of patients, the results of a recent investigation, in which MRI with MnDPDP correlated with findings of intraoperative US in 70% of the patients [32]. Of interest, in our series as well as in that report, all lesions undetected by MnDPDP-enhanced MRI and discovered at the time of surgery by intraoperative US did not exceed 1 cm in diameter.

There were some limitations to our study. Firstly, as for any multicenter trial, imaging examinations were per-

formed with a variety of equipment; hence, local differences in the quality of CT and MRI scanners as well as in the optimization of CT and MRI protocols might have affected the comparative analysis of the results. Secondly, our gold standard was provided by intraoperative US. Since we had not the opportunity to examine pathologically the entire liver, we cannot exclude false-negative results in our standard of reference. Although this limitation should not influence the results of comparative analysis of imaging modalities, absolute values of sensitivity should be regarded with caution. Thirdly, contrary to previous series in which each MR pulse sequence was evaluated separately, we compared—for the primary end point of the study—two sets of MR images, including all the precontrast and all the precontrast plus the postcontrast sequences, respectively. We recognize that this approach helps yield the best performance because visualization of a questionable area on more than one type of MR image can support the diagnosis of a focal lesion; however, this study design (simultaneous evaluation of more than one MR image obtained at the same anatomic level) simulates the everyday practice of evaluation of cross-sectional im-

ages, and made the results of the study more clinically applicable. Finally, specificity of imaging findings could not be assessed since only patients with metastases were included; hence, there were no “true negatives” on a patient-by-patient basis. On the other hand, lesion-by-lesion analysis of specificity was impaired by the presence of too few benign lesions in this series.

Conclusion

Our study showed that MnDPDP-enhanced MRI is superior to unenhanced MRI and contrast-enhanced spiral CT for the detection of hepatic colorectal metastases. Because economic pressures favor the use of less expensive imaging strategies, MnDPDP-enhanced MR imaging should be reserved to be performed in patients in whom metastases are of a pathologic type for which surgical resection or local tumor ablation have proved effective and less expensive routine screening examinations have depicted only a number of metastases which makes surgery or tumor ablation a feasible option.

References

- Brand MI, Saclarides TJ, Dobson HD, Millikan KW (2000) Liver resection for colorectal cancer: liver metastases in the aged. *Am Surg* 66:412–415
- Bolton JS, Fuhrman GM (2000) Survival after resection of multiple bilobar hepatic metastases from colorectal carcinoma. *Ann Surg* 231:743–751
- Gillams AR, Lees WR (2000) Survival after percutaneous, image-guided, thermal ablation of hepatic metastases from colorectal cancer. *Dis Colon Rectum* 43:656–6613
- Lencioni R, Cioni D, Bartolozzi C (2001) Percutaneous radiofrequency thermal ablation of liver malignancies: techniques, indications, imaging findings, and clinical results. *Abdom Imaging* 26:345–360
- Vogl TJ, Muller PK, Mack MG, Straub R, Engelmann K, Neuhaus P (1999) Liver metastases: interventional therapeutic techniques and results, state of the art. *Eur Radiol* 9:675–846
- Scheele J, Stang R, Altendorf-Hofmann A, Paul M (1995) Resection of colorectal liver metastases. *World J Surg* 19:59–71
- Sugarbaker PH (1990) Surgical decision-making for large bowel cancer metastatic to the liver. *Radiology* 174:621–626
- Mahfouz AE, Hamm B, Mathieu D (1996) Imaging of metastases to the liver. *Eur Radiol* 6:607–614
- Kondo H, Kanematsu M, Hashi H, Murakami T, Kim T, Hori M, Matsuo M, Nakamura H (1999) Preoperative detection of malignant hepatic tumors: comparison of combined methods of MR imaging with combined methods of CT. *Am J Roentgenol* 174:947–954
- Semelka RC, Cance WG, Marcos HB, Mauro MA (1999) Liver metastases: comparison of current MR techniques and spiral CT during arterial portography for detection in 20 surgically staged cases. *Radiology* 213:86–91
- Van Beers BE, Gallez B, Pringot J (1997) Contrast-enhanced MR imaging of the liver. *Radiology* 203:297–306
- Bartolozzi C, Lencioni R, Donati F, Cioni D (1999) Abdominal MR: liver and pancreas. *Eur Radiol* 9:1496–1512
- Kane PA, Ayton V, Walters HL, Benjamin I, Heaton ND, Williams R, Karani JB (1997) MnDPDP-enhanced MR imaging of the liver: correlation with surgical findings. *Acta Radiol* 38:650–654
- Clement O, Siauve N, Cuenod CA, Vuillemin-Bodaghi V, Leconte I, Frijia G (1999) Mechanisms of action of liver contrast agents: impact for clinical use. *J Comput Assist Tomogr* 23 (Suppl 1):S45–S52
- Coffin CM, Diche T, Mahfouz A, Alexandre M, Caseiro-Alves F, Rahmouni A, Vasile N, Mathieu D (1999) Benign and malignant hepatocellular tumors: evaluation of tumoral enhancement after mangafodipir trisodium injection on MR imaging. *Eur Radiol* 9:444–449
- Bartolozzi C, Donati F, Cioni D, Crocetti L, Lencioni R (2000) MnDPDP-enhanced MRI vs dual-phase spiral CT in the detection of hepatocellular carcinoma. *Eur Radiol* 10:1697–1702
- Federle M, Chezmar J, Rubin DL, Weinreb J, Freeny P, Schmiedl UP, Brown JJ, Borrello JA, Lee JK, Semelka RC, Mattrey R, Dachman AH, Saini S, Harms SE, Mitchell DG, Anderson MW, Halford HH III, Bennett WF, Young SW, Rifkin M, Gay SB, Ballerini R, Sherwin PF, Robison RO (2000) Efficacy and safety of mangafodipir trisodium (MnDPDP) injection for hepatic MRI in adults: results of the U.S. multicenter phase III clinical trials. Efficacy of early imaging. *J Magn Reson Imaging* 12:689–701
- Sahani DV, O'Malley ME, Bhat S, Hahn PF, Saini S (2002) Contrast-enhanced MRI of the liver with mangafodipir trisodium: imaging technique and results. *J Comput Assist Tomogr* 26:216–222

19. Helmberger TK, Laubenberger J, Rummeny E, Jung G, Sievers K, Dohring W, Meurer K, Reiser MF (2002) MRI characteristics in focal hepatic disease before and after administration of MnDPDP: discriminant analysis as a diagnostic tool. *Eur Radiol* 12:62–70
20. Soyer P, Levesque M, Elias D, Zeitoun G, Roche A (1992) Detection of liver metastases from colorectal cancer: comparison of intraoperative ultrasound and CTAP. *Radiology* 183:531–544
21. Soyer P, Levesque M, Caudron C, Elias D, Zeitoun G, Roche A (1993) MRI of liver metastases from colorectal cancer vs CT during arterial portography. *J Comput Assist Tomogr* 17:67–74
22. Peterson MS, Baron RL, Dodd GD III, Zajko AJ, Oliver JH III, Miller WJ, Carr BI, Bron KM, Campbell WL, Sammon JK (1992) Hepatic parenchymal perfusion defects detected with CTAP: imaging–pathologic correlation. *Radiology* 185:149–155
23. Lencioni R, Donati F, Cioni D, Paolicchi A, Cicorelli A, Bartolozzi C (1998) Detection of colorectal liver metastases: prospective comparison of unenhanced and ferumoxides-enhanced magnetic resonance imaging at 1.5 T, dual-phase spiral CT, and spiral CT during arterial portography. *MAGMA* 7:76–87
24. Low RN, Francis IR, Sigeti IS, Foo TKF (1993) Abdominal MR imaging: comparison of T2-weighted fast and contrast-enhanced fast multiplanar spoiled gradient recalled imaging. *Radiology* 186:803–811
25. Semelka RC, Shoenut JP, Ascher SM, Kroeker MA, Greenberg HM, Yaffe CS, Micflikier AB (1994) Solitary hepatic metastasis: comparison of dynamic contrast-enhanced CT and MR imaging with fat-suppressed T2-weighted, breath hold T1-weighted FLASH, and dynamic gadolinium-enhanced FLASH sequences. *J Magn Reson Imaging* 4:319–323
26. Hamm B, Mahfouz AE, Taupitz M, Mitchell DG, Nelson R, Halpern E, Speidel A, Wolf KJ, Saini S (1997) Liver metastases: improved detection with dynamic gadolinium-enhanced MR imaging? *Radiology* 202:677–682
27. Marchal G, van Hecke P, Demaerel P, Decrop E, Kennis C, Baert AL, van der Schueren E (1989) Detection of liver metastases with superparamagnetic iron oxide in 15 patients: results of MR imaging at 1.5 T. *Am J Roentgenol* 152:771–775
28. Denys A, Arrive L, Servois V, Dubray B, Najmark D, Sibert A, Menu Y (1994) Hepatic tumors: detection and characterization at 1-T MR imaging enhanced with AMI-25. *Radiology* 193:665–669
29. Bellin MF, Zaim S, Auberton E, Sarfati G, Duron JJ, Khayat D, Grellet J (1994) Liver metastases: safety and efficacy of detection with superparamagnetic iron oxide in MR imaging. *Radiology* 193:657–663
30. Seneterre E, Taourel P, Bouvier Y, Pradel J, van Beers B, Daures JP, Pringot J, Mathieu D, Bruel JM (1996) Detection of hepatic metastases: ferumoxides-enhanced MR imaging vs unenhanced MR imaging and CT during arterial portography. *Radiology* 200:785–792
31. Hagspiel KD, Niedl KFW, Eichenberger AC, Weder W, Marincek B (1995) Detection of liver metastases: comparison of superparamagnetic iron oxide-enhanced and unenhanced MR imaging at 1.5 T with dynamic CT, intraoperative US, and percutaneous US. *Radiology* 196:471–478
32. Mann GN, Marx HF, Lai LL, Wagman LD (2001) Clinical and cost effectiveness of a new hepatocellular MRI contrast agent, mangafodipir trisodium, in the preoperative assessment of liver resectability. *Ann Surg Oncol* 8:573–579